

From Kondo semiconductor to a singular non-Fermi liquid via a quantum critical point: The case of $\text{CeRhSb}_{1-x}\text{Sn}_x$

J. Spalek,¹ A. Ślebarski,² J. Goraus,² L. Spalek,³ K. Tomala,¹ A. Zarzycki,¹ and A. Hackemer⁴

¹Marian Smoluchowski Institute of Physics, Jagiellonian University, Reymonta 4, 30-059 Kraków, Poland

²Institute of Physics, University of Silesia, Uniwersytecka 4, 40-007 Katowice, Poland

³The Henryk Niewodniczański Institute of Nuclear Physics, Polish Academy of Sciences, Radzikowskiego 152, 31-342 Kraków, Poland

⁴Institute for Low Temperature and Structure Research, Polish Academy of Sciences, Okólna 2, 50-950 Wrocław, Poland

(Received 3 June 2005; revised manuscript received 8 August 2005; published 14 October 2005)

We discuss and interpret the properties of the $\text{CeRhSb}_{1-x}\text{Sn}_x$ systems in the concentration interval $0 \leq x < 0.2$. For $x \approx 0.13$ a quantum critical point has been observed by us recently and separates the Kondo-insulator (KI) from the metallic non-Fermi-liquid (NFL) state. We present the temperature dependence of the resistivity, the ac and dc magnetic susceptibilities, the specific heat, and the magnetization data through the critical concentration regime $x \sim 0.12-0.13$, as well as provide their discussion in terms of the transition from the nonmagnetic (Kondo-lattice) insulator to a weakly magnetic and singular non-Fermi liquid. The difference between the Kondo-lattice and the Mott-Hubbard semiconductors at temperature $T > 0$ is emphasized. Also, the difference between those two types of insulating states is discussed. On the basis of the experimental results we propose a schematic phase diagram on the plane $T-x$ and demonstrate the rationale for the existence of the quantum critical point separating KI and NFL phases. Namely, we propose that the metallization of the insulating Kondo lattice in terms of the collective spin-singlet Kondo-lattice state destruction and a concomitant delocalization of the $4f$ electrons, within an effective f -band model of correlated electrons undergoing the phase transition to the insulating state.

DOI: [10.1103/PhysRevB.72.155112](https://doi.org/10.1103/PhysRevB.72.155112)

PACS number(s): 71.27.+a, 72.15.Qm, 71.30+h

I. INTRODUCTION

The purpose of this paper is to discuss in detail and interpret a type of a quantum critical behavior for $\text{CeRhSb}_{1-x}\text{Sn}_x$, which has been proposed by us recently.¹ Namely, we determine how a semiconducting system with the Kondo gap transforms at $x \approx 0.12$ into a non-Fermi-liquid (NFL) metallic state. Both the Kondo gap and the corresponding critical exponents in the NFL phase are obtained as a function of the Sn content x . In this manner, we demonstrate the existence of a quantum critical point, which appears at the Kondo insulator-non-Fermi-liquid boundary, as well as characterize the critical behavior on the metallic side.

The quantum critical phenomena are intensively studied in various correlated electron systems.^{2,3} This means that singularities of the macroscopic physical properties are observed with temperature $T \rightarrow 0$ for quantities such as the magnetic susceptibility χ , the linear specific-heat coefficient, $\gamma \equiv C/T$, and the electrical resistivity, $\rho(T)$. In other words, these properties do not display the low- T dependence characteristic of the Landau theory of Fermi liquids.⁴ One can also say that the theory based on the paradigm which started with the Sommerfeld and Landau low- T expansions of physical quantities fails when the system approaches the quantum critical point (QCP). In the simplest narrow-band system the quantum criticality arises from a competition between the two energy scales: one of them arises from the kinetic (band) energy of the itinerant carriers, $\epsilon_k < 0$, the other is associated with the repulsive Coulomb interaction $\epsilon_{e-e} > 0$, which favors localized-lattice states. In such a manner, the Mott-Hubbard localization has been explained in the narrow-band systems⁵ when $|\bar{\epsilon}_k| \sim \bar{\epsilon}_{e-e}$.

In the case of heavy-fermion systems, a very narrow band of correlated states involving an itineracy of f electrons is formed^{4,6} on the energy scale $T_K = 10-100$ K, which can be relatively easily destroyed by either thermal motion at temperature $T \geq T_K$ or by atomic disorder, or else by external influence such as the applied pressure or magnetic field. A particularly interesting situation arises when the energy calculated in the mean-field approximation is comparable to the energy of quantum fluctuations. Under this circumstance, a true quantum critical behavior should be observed without the external influence, when temperature $T \rightarrow 0$. In this respect, it is our purpose to discuss both experimentally and theoretically the Kondo-semiconductor lattice which becomes unstable against metallization.

The second rationale behind the present paper comes from our attempt to examine the evolution of the Kondo-lattice insulating state by varying the system carrier concentration. This should allow us to see the destruction of the Kondo-type state in the lattice case if the carrier concentration, when lowered intentionally, crosses a critical concentration for the periodic Kondo-singlet state formation. In this respect, an elementary argument (Nozieres⁷) showed that in the lattice system there may not be enough carriers to compensate completely the f -electron magnetic moment due to Ce or U. A refined analysis demonstrates,^{8,9} that if f electrons are almost localized but still itinerant, they partly autocompensate each other by both obeying the Pauli principle, and creating anti-ferromagnetic kinetic-exchange interaction with their neighbors. The resultant picture coming from our results is that at the critical concentration $x_c \approx 0.12$ the singlet Kondo-state [characterized by $\chi(T \rightarrow 0) \rightarrow 0$ for $x \leq x_c$] is destroyed and the magnetic state is approached, since for $x \geq 0.13$,

$\chi(T \rightarrow 0) \rightarrow \infty$. We believe that this type of behavior is unique and is clearly observed here even under the presence of substitutional atomic disorder (i.e., replacement of Sb with Sn).

The structure of the paper is as follows. In Sec. II we provide experimental details of the synthesis and measuring techniques. In Sec. III we present overall properties of mixed systems $\text{CeRhSb}_{1-x}\text{Sn}_x$, with $x < 0.2$, and we connect the temperature dependence of the resistivity to that of the magnetic susceptibility. This connection represents a *type of scaling* $\chi\rho = \text{const}$ unique for the Kondo semiconductors at intermediate low temperatures. In Sec. IV we present the magnetization data and display the temperature dependence of the specific heat for the critical concentration $x = 0.13$. In Sec. V we discuss in detail the physical implications of the results and determine the main features of the phase diagram on the T - x plane. Finally, in Sec. VI we interpret theoretically the results by combining the f -electron itineracy, the effective Kondo coupling, and the antiferromagnetic exchange, all of which represent comparable energy scales.

II. EXPERIMENTAL DETAILS

CeRhSb and CeRhSn master samples were first prepared by arc melting the weighted amount of each component. The dilute $\text{CeRhSb}_{1-x}\text{Sn}_x$ alloys were then prepared by diluting the master alloys. To ensure homogeneity, each sample was turned over and remelted several times and then annealed at 800°C for 2 weeks. The samples were carefully examined by x-ray diffraction analysis and found to be single phase (with the orthorhombic $\epsilon\text{-TiNi}_x\text{Si}_{1-x}$ structure, space group $Pnma$). The stable samples are synthesized only in the $0 \leq x < 0.20$ concentration range and the again for $x \geq 0.80$; the latter systems will not be discussed here.¹⁰

A standard four-terminal ac technique was used to measure the resistance of each sample, from which the resistivity was calculated by multiplying it with the shape factor. The absolute resistivity was obtained within $\pm 3\%$ due to the uncertainty in the shape factor. However, the relative resistivity can be measured to an accuracy of $\sim 1 \times 10^{-4}$.

The magnetic susceptibility was measured in the 2–300 K regime by use of a commercial ac Lake-Shore susceptometer. The amplitude of the excitation field was 1 mT at a fixed frequency of 10 kHz.

dc susceptibility and magnetization measurements were made using a commercial superconducting quantum interference device magnetometer (Quantum Design) for temperatures in the range 1.8–300 K.

Specific-heat measurements have been performed in a fully adiabatic calorimeter between 2.7 K and 30 K.

III. ELECTRICAL RESISTIVITY, MAGNETIC SUSCEPTIBILITY, AND THEIR UNIVERSAL RELATION IN THE INSULATING STATE: $x \leq 0.12$

A. Resistivity

In Figs. 1(a) and 1(b) we display the temperature dependence of the electrical resistivity for the samples with $x < 0.12$ (a) and $0.12 \leq x \leq 0.16$ (b). The curves in Fig. 1(a) exhibit a well defined activated behavior where

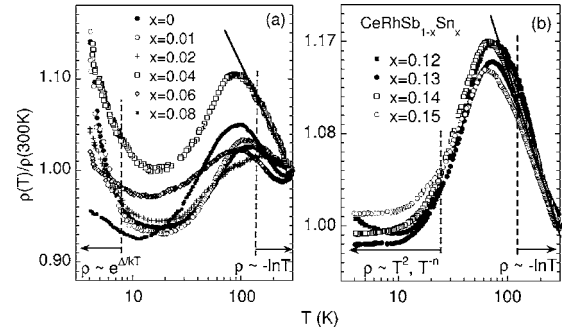


FIG. 1. Temperature dependence of the relative resistivity ρ for $\text{CeRhSb}_{1-x}\text{Sn}_x$ systems for $x \leq 0.08$ (a) and $0.12 \leq x \leq 0.15$ (b). The regimes, where $\rho(T) \sim \exp(\Delta/T)$, $\sim \ln T$, and $\sim T^\epsilon$ are marked in the corresponding T intervals. The parametrization of the data is listed in Table I.

$\rho \sim \exp(\Delta/T)$ is the low-temperature regime that is characteristic of a nondegenerate semiconductor, with the activation energy $\Delta = \Delta(x)$ listed in Table I. In this paper we are interested only in the temperature regime below the resistivity maximum, i.e., when the *quantum coherence effects* connected with a formation of heavy carriers set in. Above, the high-temperature ρ maximum, which appears in the range of $T_{max} \sim 50\text{--}70$ K depending on the concentration x , a well defined logarithmic dependence with a negative slope is observed. The resistivity maximum results from a competition between quantum coherence (i.e., itineracy of $4f$ electrons due to the hybridization with $5d$ - $6s$ carrier states and setting in upon cooling) and the thermal disorder acting as a *decoherence factor* breaking the hybridization-induced coherence and, in effect, localizing the $4f$ electrons for $T > T_{max}$. Above T_{max} the magnetic susceptibility approaches gradually with further T increasing the Curie-Weiss, law for $4f^1$ localized moments on Ce.

For $x > 0.12$ [see Fig. 1(b)] a well defined metallic behavior $\rho \sim \rho_0 + AT^2$ is established for not too low temperatures ($10 < T < 30$ K). Therefore, we observe the transformation from a semiconductor to a correlated metal appearing in the interval of x between 0.12 and 0.13. The most interesting question that appears at this point is whether this gradual gap disappearance ($\Delta = 0$ for $x > 0.12$) is associated with a phase transformation of the electronic subsystem. This question will be addressed next.

B. Magnetic susceptibility

To determine the nature of the semiconducting phase for $x \leq 0.12$ and $T \rightarrow 0$ we have shown in Figs. 2(a) and 2(b) the temperature dependence of the magnetic susceptibility χ . The impurity contribution of the Curie type (yC/T), with the value of the Curie constant $C = 0.807$ K emu/mol for Ce^{3+} , has been subtracted from the raw data, with $y \leq 0.008$, depending on the sample. Under these circumstances, the spin susceptibility $\chi \rightarrow 0$ as temperature decreases starting from about $T \approx 20$ K. This dependence speaks in favor of a nonmagnetic (spin-singlet) nature of the ground state for the samples with $x \leq 0.12$. We interpret this behavior as a clear sign of the Kondo insulating state, since the $4f^1$ magnetic

TABLE I. ac susceptibility and the resistivity parametrizations of the $\text{CeRhSb}_{1-x}\text{Sn}_x$ samples in the regime $x \leq 0.16$.

x	$\chi = \chi_0 + C/(T - \theta)$			$\chi = aT^{-m}$		$\rho = \rho_0 \exp(\Delta/T)$ Δ (K)	$\rho = \rho_0 + AT^2$ A ($10^2 \mu\Omega \text{ cm K}^{-2}$)	$\rho - AT^2 \sim T^{-n}$ $10^3 n$
	χ_0 (10^3 emu/mol)	θ (K)	C (emu K/mol)	$10^3 a$	m			
0		-123.8	0.54			6.7		
0.01		-120	0.40			1.80		
0.02		-149.5	0.47			0.64		
0.04		-67.8	0.50			0.70		
0.06		-81.7	0.53			0.30		
0.08		-97.9	0.84			0.22		
0.10						0.10		
0.12		-104.9	0.92			0.10		
0.13	2.6	-7.0	0.043	6.0	0.17		1.78	8.0
0.14	1.7	-9.1	0.021	4.3	0.17		1.69	2.8
0.15							1.20	2.7
0.16	3.5	-7.6	0.038	6.0	0.09		0.186	1.3
0.19	4.4	1.7	0.028	8.8	0.12		5.10	$\rho - AT^2 = 0$
							($T < 25$ K)	
		15 < T < 80 K		$T < 10$ K		$T < 10$ K	10 ≤ T ≤ 30 K	$T < 10$ K

moments of Ce^{3+} ions have been reduced essentially as $T \rightarrow 0$ (i.e., a collective spin-singlet Kondo-lattice state is formed). On the other hand, the divergent character of χ shown in Fig. 2(b) for $x > 0.12$ (cf. also Table I) is attributed to the quantum critical behavior $\chi = aT^{-m}$ in the whole metallic (non-Fermi liquid) regime $x < 0.20$, which will be dealt with in the next section. Also, an additional weak hump in $\chi(T)$ is detectable at $T \sim 10$ K.

One should note that in the KI state [Fig. 2(a)] χ reaches maximum first before diving into the $\chi \rightarrow 0$ limit with further decreasing T . The presence of this maximum can be understood when we reflect on the increasing χ with the increasing T . Then, the maximum in χ is reached at a temperature, where the collective singlet state is destroyed by the thermal

motion and the f spins respond to magnetic field. Note also that the maximum is dependent on x (see Table II) and evolves into the $\chi \rightarrow \infty$ singularity for $x \geq 0.13$. This means that then the magnetic critical state at $T \rightarrow 0$ is approached when the spin-singlet state cannot be formed anymore and seems to survive for all concentrations $x < 0.20$, i.e., in the concentration range, in which the samples can be synthesized. The position of the χ maximum determines then the effective binding energy of $4f$ spins into a collective singlet and is reduced by about 40% when the critical concentration $x = 0.12$ is reached. One should note that $x > 0T_m \gg 2\Delta$, where 2Δ is the binding energy per carrier. This means that the $4f$ spins are bound roughly to $N \equiv T_m/(2\Delta)$ carriers in the KI state. If $x = 0.02$, $2\Delta = 1.3$ K, and $N \sim 12$ and carriers for $x = 0$, then $N \sim 1$. This interpretation will be taken on later. However, one should note that while at $T = T_{max}$ the f electrons acquire itineracy (as seen by the appearance of T^2 term in the resistivity), those mixed electrons reach a collective spin-singlet state for $T < T_m \ll T_{max}$. So, we can say that we have a mixed very-narrow-band behavior in the regime $T_m < T < T_{max}$ and a true Kondo-lattice for $T < T_m$. Does that mean that the f electrons localize back again for $T < T_{max}$?

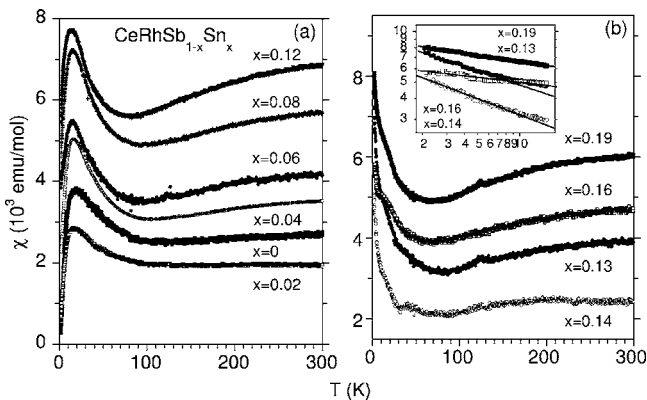


FIG. 2. Temperature dependence of the ac susceptibility for $\text{CeRhSb}_{1-x}\text{Sn}_x$ systems with $x \leq 0.12$ (a) and $0.12 < x \leq 0.19$ (b). A qualitative difference of $\chi(T \rightarrow 0)$ behavior on the two panels should be observed and attributed to the quantum critical point presence located between $x = 0.12$ and $x = 0.13$. The inset illustrates the scaling $\chi \sim T^{-m}$ on the double logarithmic scale, observed in the regime $\Delta T = 1.8 - 12$ K.

TABLE II. Concentration x dependence of the temperature T_m , at which ac χ reaches the maximum in the Kondo semiconducting state [see Fig. 2(a)].

x	T_m in K
0	18.6
0.02	16.6
0.04	15.9
0.06	14.8
0.08	15.3
0.12	13.7

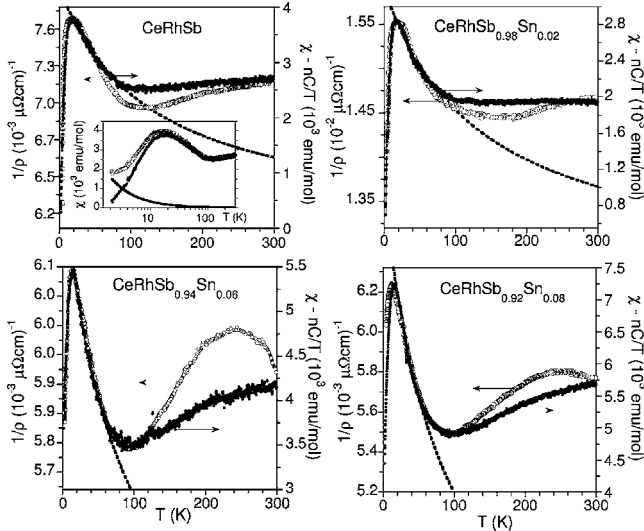


FIG. 3. The scaling $1/\rho$ vs χ in the Kondo insulating regime. The dashed lines express the Curie-Weiss parametrization (for values of parameters see Table I) in the limited temperature range. The impurity contribution ($\gamma C/T$) has been subtracted from the raw χ data, but not in the resistivity.

This *reentrant* localized behavior will be discussed below.

C. Universal scaling law: $\rho\chi=\text{const}$

An additional very interesting property has been observed in the semiconducting state. Namely, a simple and universal type of scaling between the inverse resistivity and the susceptibility can be observed for temperatures $T \leq 60$ K for all the samples with $x \leq 0.12$; this relation is plotted in the panel in Fig. 3. In the inset to this figure we show the raw χ data (open circles), those with the Curie term ($\gamma C/T$) subtracted from them (full circles), as well as the $\gamma C/T$ contribution (solid line); this is to show that even the raw data exhibit the χ decrease upon cooling. The dashed lines in the figures express the Curie-Weiss parametrization of the χ data for temperatures above the maximum (for values of the corresponding parameters, see Table I).

The scaling law illustrated for individual samples can be set on more formal ground by plotting ρ vs χ^{-1} for different samples, as detailed in Fig. 4. In the inset we have plotted the product $\rho\chi$; it remains practically unchanged for the samples with $x \leq 0.06$, i.e., in the regime of relatively weak disorder.

With this type of scaling we prove that the resistivity is related to the magnetic degrees of freedom. Such a relation provides an additional and quite universal characteristic of the Kondo semiconductors; it is certainly absent for the magnetic semiconductors, which are Mott-Hubbard systems. Additionally, since the corresponding impurity contribution has not been subtracted from the $\rho(T)$ data, we can then ascribe the deviation from the scaling to this difference in the procedure of treating χ vs ρ data. The relation $\chi \sim \rho^{-1}$ and the fact that $\chi \rightarrow 0$ with $T \rightarrow 0$ have immediate implications concerning the nature of the Kondo insulator. Namely, the susceptibility should vanish at $T=0$ if we have the band insulator (the full band) or if the singlet spin state of the Kondo

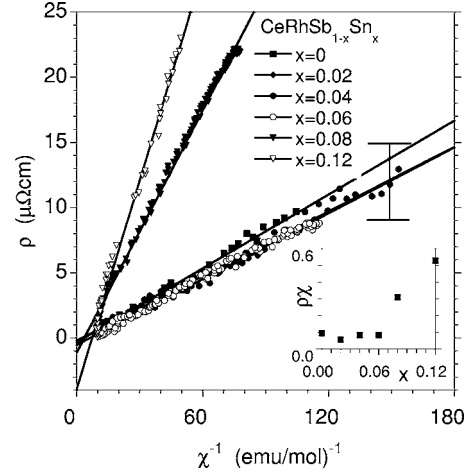


FIG. 4. Linear scaling law between the resistivity ρ and the susceptibility χ for the nonvanishing Kondo gap. The values of χ and ρ for different x are shifted to the zero values at the minimal positions. Inset: the value of $\rho\chi$ as a function of x ; it stays the same as in the regime of the relative weak disorder, $x \leq 0.06$.

lattice is realized. These two possibilities are drawn schematically in Figs. 5(a) and 5(b). The physical distinction between the two possible states is discussed below. However, in accordance with what has been said above, the band insulator (i.e., the system with an even number of valence electrons per formula¹) should become metallic for $x > 0$ if disorder is not the primary cause of the insulating state. The fact that the system remains semiconducting up to $x=0.12$ suggests that the collective Kondo effect is important. In the following section we will concentrate on the quantum critical behavior, as well as discuss in detail the metallic phase for $x \geq 0.13$.

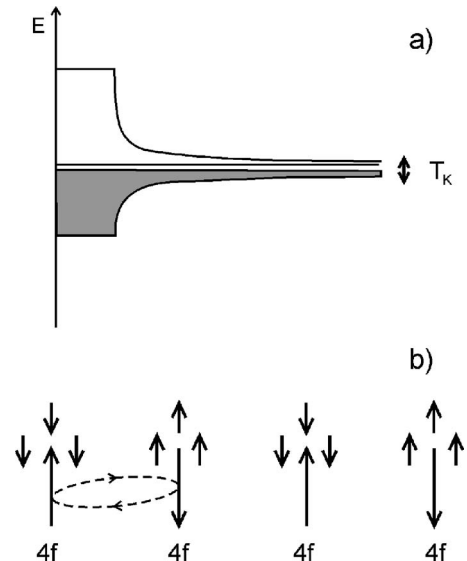


FIG. 5. Schematic representation of the Kondo insulator as either a correlated and hybridized narrow-band insulator (a) or as a collective spin singlet state $S_{tot}=0$ (b). The actual situation is that between the simple mean-field slave-boson result (Refs. 4, 8, and 9) (a) and the more refined picture (b), if f electrons are localized.

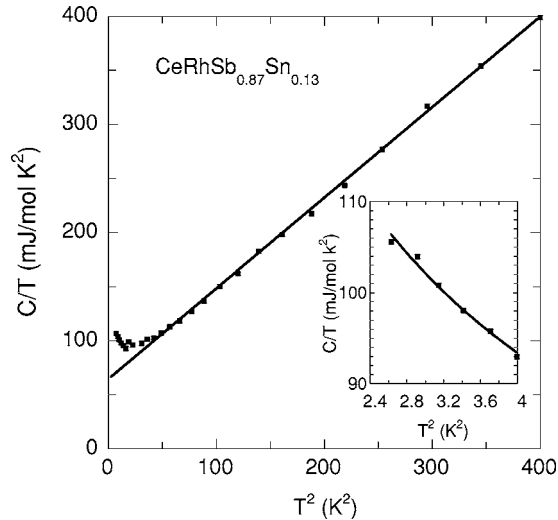


FIG. 6. Temperature dependence of the specific heat for the sample with $x=0.13$. The solid line is the fit to the dependence $C/T = \gamma + \beta T^2$. The inset shows the deviation from the fitted dependence, as well as the fit $C/T \sim T^{-0.3}$.

IV. PROPERTIES IN THE METALLIC REGIME: $x \geq 0.13$

A. Critical behavior

The critical behavior of χ is extracted from the temperature dependences shown in Fig. 2(b), where the dependence $\chi = aT^{-m}$ has been fitted to the ac data, with the parameters listed in Table I. The divergence of $\chi(T \rightarrow 0)$ means that the system reaches a magnetic moment bearing a phase-transition point at $T=0$. This divergence at the weak ferromagnetism threshold is observed for all the samples listed with $x \geq 0.13$. The samples were checked and are single phased. The $\chi(T)$ curves exhibit an additional slightly abnormal behavior around $T \sim 10$ K. Previously,¹ we have detected a weak singular behavior in $\rho(T)$ for the sample with $x=0.13$. The χ divergence for $T \rightarrow 0$ for all the samples suggests that we may have a *singular* non-Fermi-liquid phase, i.e., with a line of singularities at $T=0$ along $x \geq 0.13$ axis. However, a further checkout of this suggestion at much lower temperatures is required.

To confirm the critical character of the behavior, we have shown in Fig. 6 the temperature dependence of the specific heat for the $x=0.13$ sample. The solid line expresses the dependence $C_p = \gamma T + \beta T^3$, with $\gamma = 63$ mJ/K² mol. The deviation of the specific heat for $T \rightarrow 0$ from the straight-line behavior should be noted; it is displayed in detail in the inset. The singular part can be parametrized by the dependence $C_p/T = bT^{-s}$, with $s \approx 0.3$. This behavior marks the divergence of the linear specific-heat coefficient γ for $T \rightarrow 0$. This divergence must be associated with the Fermi surface instability when entering the KI phase, i.e., the quasiparticle mass m^* divergence, since $\gamma \sim m^*$.

One should note that the singular behavior $C_p/T \sim T^{-s}$ evolves upon lowering temperature from the Fermi-liquid state of moderately heavy quasiparticles with $\gamma(0) = 63$ mJ/K² mol. At the same time (cf. Table I, column 8) the deviation from the Baber-Landau-Pomeranchuk law

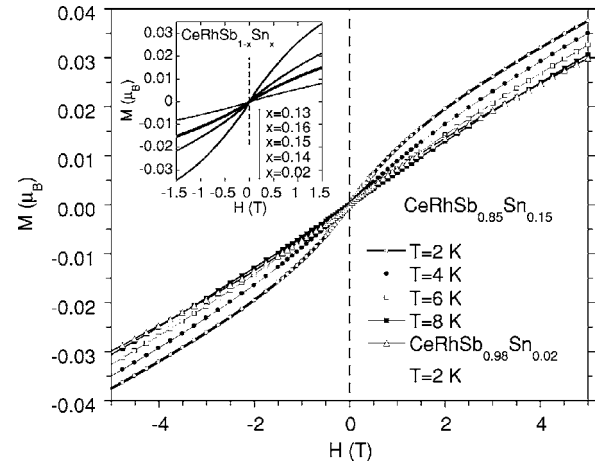


FIG. 7. Magnetization curves for the metallic samples ($x \geq 0.13$) and a comparison with that for the Kondo insulator with $x=0.02$. In the inset we present the $M(H)$ data for x specified and $T=2$ K.

$\rho(T) = \rho_0 + AT^2$ is observed (*ibid.*, column 9). This means that the NFL state emerges gradually from FL state for $T < 10$ K. Such an emergent singular behavior with $T \rightarrow 0$ is very easy to rationalize. Namely, if we try to estimate the entropy contribution due to the singular behavior at low T we will have

$$S(T) = \int_0^T \frac{C_p dT}{T} \approx \int_0^T (bT^{-0.3} + \gamma) dT = \frac{3}{2} bT^{0.7} + \gamma T.$$

Taking for $x \approx 0.13$ the value $b = 143.6$ mJ/K^{1.7} mol, we observe that for $T \leq 2$ K the singular part of C/T overcomes the Fermi-liquid contribution γT . In other words, the number of accessible states for fluctuations is enlarged and depends on an anomalous manner on temperature.

B. Magnetic properties

In Fig. 7 the overall magnetization curves for the metallic samples ($x \geq 0.13$) and for the $x=0.02$ sample are shown. In the inset we specify the curves for sample with x specified and for $T=2$ K. To systematize those data we have redrawn them as a function of H/T in Fig. 8. The curves are roughly converging for $(H/T) \rightarrow 0$, but exhibit a diverse character with the increasing field (above ~ 2 kOe), which means that the magnetic moment cannot be attributed to the impurities. A fitting of the Brillouin curve with a variable spin has been unsuccessful. Likewise, the drawing of the Arrott plots is inconclusive. In effect, these curves represent the behavior for an itinerant magnetic phase, with a very small magnitude, originating from the exchange interactions and, possibly, a strong anisotropy, since the curves do not saturate in the accessible field up to 5.5 T. Obviously, in the small-field regime $M = \chi H$, so the scaling with H/T implies that $M = (\chi T) H/T$ and χT varies slowly with T . The character of the deviation from the straight-line dependence means that a molecular field ($J_{ex} M$) acts on the magnetic spins. This is because the magnetization curve should be a function of the argument $H_{eff}/T = (H + J_{ex} M)/T$, where H_{eff} is the effective

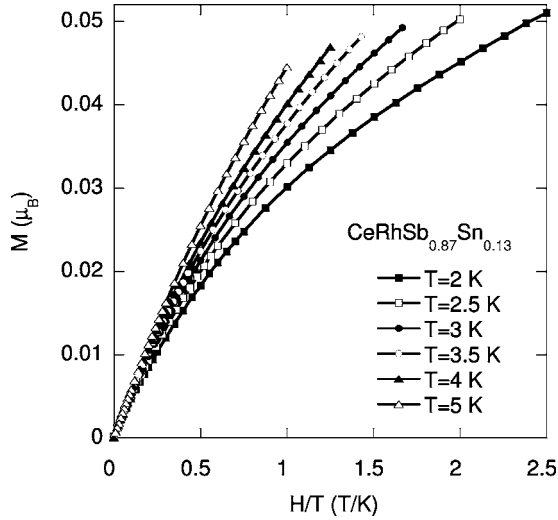


FIG. 8. Scaling of M data with H/T . The data are roughly convergent with $H \rightarrow 0$. The bending of the curves rules out the impurity nature of the moment origin.

field and J_{ex} is the exchange integral. One additional feature of our results should be mentioned. Namely, the dc magnetic susceptibility data for the samples with $x \geq 0.13$ show as a rule a higher value of the exponent m , as shown in Fig. 9, when compared to their ac correspondants. The parameters of the fitting to the law $\chi = aT^{-m'}$ in this case are listed in Table III. The results are the same within the error for both the field cooled (FC) and zero-field cooled (ZFC) measurements, which means that there is no spin-glass behavior present for $T \geq 2$ K. The exact nature of the difference between the values m and m' of the exponents when determined, respectively, from the ac and dc methods, is not understood at this moment. However, a small hysteresis observed for $T \lesssim 4$ K speaks in favor of the weakly spin-polarized phase, as discussed below.

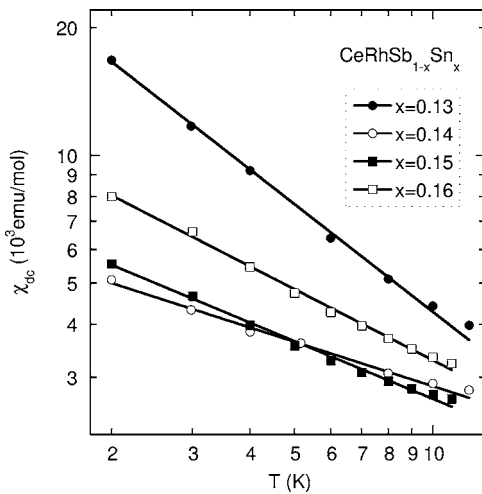


FIG. 9. The divergent behavior of the susceptibility determined by dc ZFC measurements for the metallic samples. The solid lines represent the fitting to the dependence $cT^{-m'}$ and the values of the parameters are collected in Table III.

TABLE III. $\text{CeRhSb}_{1-x}\text{Sn}_x$; a and m' parameters for the best fits of an equation $\chi = aT^{-m'}$ to the dc susceptibility data obtained for $T < 7$ K in the metallic regime $x \geq 0.13$ (see also Fig. 8).

x	$\chi = cT^{-m'}$ $10^3 c (\text{emu mol})$	m'
0.13	29.96	0.84
0.14	7.56	0.35
0.15	11.83	0.45
0.16	6.39	0.55

V. FURTHER RATIONALIZATION OF THE RESULTS

From the evolution of the x dependences of χ and ρ the following physical picture clearly emerges and can be summarized under the following headings. First, the activated behavior of the conductivity is related to the fact that the nonzero carrier concentration n_C for $x \leq 0.12$ is created by their thermal excitation across the Kondo gap. While the energy $\Delta < T_m$ is connected with the breaking of the binding into a collective singlet of individual carriers, the value T_m refers to the binding energy of $4f$ electrons into such a singlet. As the multiple carriers are bound to a single $4f$ spin, it is clear that $T_m > 2\Delta$ for $x > 0$. Also, the dependence $\rho \sim \exp(\Delta/T)$, characteristic of a nondegenerate semiconductor, is obeyed even for temperature $T \geq \Delta$, in agreement with the well known experimental fact that the Kondo semiconductors are the systems with a low carrier concentration. Likewise, the magnetic susceptibility $\chi \sim n_C$, as the magnetic moments appear from the spin-singlet bound state with $\chi \approx 0$ (the orbital diamagnetism is very small). An elementary analysis shows that for those thermally activated quasiparticles $\rho = m^*/(n_C e^2 \tau)$, so that $\rho \chi = \text{const}$, if only the carrier lifetime τ and the effective mass m^* do not change appreciably with either T or x (this is the case for $x \leq 0.06$). In this manner, the observed scaling law $\rho \sim \chi^{-1}$ can be easily understood, at least in the low-temperature regime $T \leq 10$ K. Also, for $T > T_m$ the free $4f$ moment due to Ce emerges and hence the susceptibility is described, albeit in a limited temperature interval $T \leq 80$ K, in terms of Curie-Weiss law (cf. the dashed line in Fig. 3). However, representation of χ^{-1} is only a phenomenological parametrization since the Curie-Weiss law is physically sound only in the asymptotic regime $T > |\theta|$, which is not the case here (for values of θ see Table I, column 3). At still higher temperature valence fluctuations induced thermally become important and lead to a broad hump.¹¹

Second, the system is insulating for $0 \leq x \leq 0.12$. This means that the collective bound Kondo-lattice insulating state survives for $T < T_m$ up to $x = 0.12$. The role of atomic disorder should not be regarded as crucial, since the localized carriers (holes) introduced upon the substitution would form paramagnetic centers, whose number should grow $\sim x$, which is not observed. Conversely, all the available carriers form a collective spin-singlet state. Furthermore, since the substitution of Sn for Sb diminishes the number of valence electrons by one and the metallicity is not observed for $x < 0.13$, the KI state is that drawn in Fig. 5(b), i.e., the electrons freeze

into the lattice of Kondo singlets. Otherwise, it would be very difficult to understand the mechanism of trapping the individual holes created by the substitution and their nonmagnetic state. However, one must realize that $\text{CeRhSb}_{1-x}\text{Sn}_x$ has $(18-x)$ valence electrons (including the f electron) so the necessary condition for the appearance of the band insulator is met at $x=0$. For $x>0$ the Kondo state enforces then the electron localization. Thus we have a combined band-Kondo behavior for $0<x<0.13$.

Third, the maximum in χ at $T=T_m$ reflects, as said above, the fluctuations destroying the collective singlet in the system and creates net magnetic moments due to f electrons with the effective exchange interaction between them of the magnitude $J_{ex}/k_B \sim 10$ K. In effect, we have three coinciding scales of energies $2\Delta(0)$, T_m , and J_{ex} . Note again, that $2\Delta(0)$ is the binding energy of carriers into the singlet, whereas T_m is the corresponding binding energy of the f electron. The fact that T_m is reduced by 40% when x changes from $x=0$ to $x=0.12$ means that the Kondo-singlet destruction with the increasing x is due to insufficient carrier concentration, not due to changing strength of the Kondo coupling, since we are in the whole interval in the insulating state. Thus, the evolution with x complements the *Doniach scenario*¹² which takes place at a constant carrier concentration when the pressure is applied.¹³ Additionally, this scenario should be modified to account for the itineracy of $4f$ electrons when the collective Kondo-singlet state is destroyed for either $T>T_m$ or $x \geq x_C$. In other words, our results indicate clearly that for $T_{max} > T \geq T_m$, the f electrons become itinerant until the temperature $T=T_{max}$ point is reached, at which the quantum coherence of the itinerant $4f$ electron states is terminated. Below $T<T_{max}$ hybridization of $4f$ with conduction-band states is strong enough to sustain their itineracy, whereas for $T<T_m$ the collective spin-singlet state is formed and causes a second $4f$ -electron localization upon cooling. In this picture, the system would remain a heavy-fermion metal down to $T=0$ if a collective spin-singlet state could not be formed due to an insufficient number of the valence electrons. The Kondo semiconducting state can be thus regarded as a *reentrant localized f -electron behavior* upon cooling the system. A reverse reentrant sequence of states appears in Mott-Hubbard systems such as V_2O_3 .¹⁴ The localization at $T>0$ in the Mott-Hubbard systems is caused by the circumstance that the entropy of the localized paramagnetic state (with thermally fluctuating magnetic moments $S=R \ln 2$) is larger than that in the metallic state ($S \sim \gamma T$). Here, the opposite is true and hence the sequence of phases vs T is reversed.

Finally, and probably most importantly, $\chi(T)$ seems to diverge for all metallic samples possible to synthesize, i.e., for $x<0.20$. The samples are single-phase systems. This means that the observed divergent behavior of $\chi(T \rightarrow 0)$ for $x \geq 0.13$ defines a *singular* non-Fermi liquid exhibiting a line of quantum critical points. Additionally, the C/T divergence for $T \rightarrow 0$ defines the effective mass divergence and the onset of magnetism, since the density of states at the Fermi level $\rho(\epsilon_F)$ becomes divergent with $T \rightarrow 0$.

Parenthetically, it would be extremely interesting (and important) to extend our measurements to very low temperatures to check, among others, if the critical exponents remain

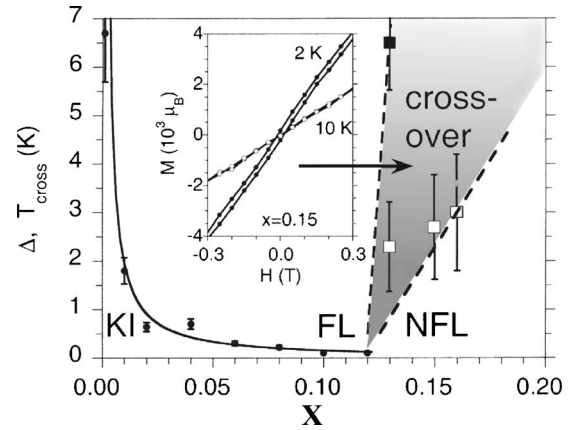


FIG. 10. Schematic phase diagram for $\text{CeRhSb}_{1-x}\text{Sn}_x$ systems. The solid circles mark the values of the Kondo gap $\Delta(x)$. The full square marks the deviation point from the T^2 dependence of resistivity for $x=0.13$, whereas the open squares mark the disappearance points (T_c) of a very weak hysteresis on the magnetization curves. In the inset we draw the temperature dependence of part of the typical hysteretic behavior, here plotted for the $x=0.15$ sample.

the same as those determined here. This is planned as the next step in our investigations.

On the basis of the experimental data and the above discussion a schematic phase diagram can be drawn, as shown in Fig. 10. The solid line (guide to eye) on the left parametrizes the measured values of the Kondo-lattice gap $\Delta(x)$; its flat part may be partly caused by the disorder. The inset shows a residual magnetic hysteresis observed at low temperatures. We attach this hysteresis to the presence of a very small moment in the system. Here, a remark is in place. We cannot separate the sample remanence from the superconducting magnet residual moment. However, we believe that this property can be ascribed to the sample, since it disappears at a temperature far below that for the superconductor-normal metal transition for the solenoid material. Also, the shaded area is the crossover region from either KI or Fermi liquid (FL) states to the non-Fermi (non-Landau) metallic phase NFL. The fact that the critical exponent for $x=0.13$ for the specific heat is $\nu=0.3 \sim 1/3$ means that this critical point is not of the same type as either the liquid-gas or PM \rightarrow PI (Ref. 14) transition, for which no symmetry change occurs at the critical point. Conversely, the metallic phase is regarded as a very weakly magnetic phase, but the exact nature of this magnetism needs further study by NMR and other techniques at lower temperatures.

VI. THEORETICAL INTERPRETATION: KONDO-INSULATOR METALLIZATION

A. Difference with the Mott-Hubbard systems

Apart from the interest in the $\text{CeRhSb}_{1-x}\text{Sn}_x$ critical behavior near $x \approx 0.12$, we should first compare briefly the present system with the classic Mott-Hubbard systems such as doped V_2O_3 systems, $\text{V}_{2-x}\text{Cr}_x\text{O}_3$,¹⁴ and $\text{NiS}_{2-x}\text{Se}_x$.¹⁵ The difference between the Mott-Hubbard systems and the hybridized-band systems is schematically drawn in Fig. 11.

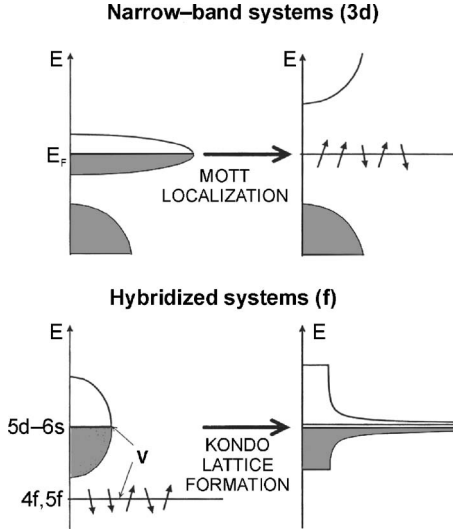


FIG. 11. Schematic representation of the Mott-Hubbard localization (top line) and the Kondo-lattice insulator formation (bottom part). V denotes the magnitude of the local hybridization between the $4f$ and the conduction (c) states. The bottom-right part has been refined in 5(b) in terms of a collective Kondo-lattice singlet state, when f electrons localize for $T < T_m$.

The first are $3d$ narrow-band systems, in which the Mott-Hubbard localization takes place as a function of either doping or temperature and is associated with the narrow-band instability and the concomitant transformation of an almost localized Fermi liquid into the lattice of localized moments. It is important that the band filling per atom is an even number (in the simplest case, a single narrow band is half-filled, as shown in the top panel). The situation for the doped systems is much more complicated due to the presence of the atomic disorder. It is important to note that the insulating phase is magnetic (very often antiferromagnetic), as the localized electrons in the localized state are not spin paired. The presence of the antiferromagnetism, also in the metallic state, obscures the detection of the predicted quantum critical point¹⁴ at the paramagnetic metal (PM)-paramagnetic insulator (PI) threshold at $T=0$. Instead, the classical critical point at $T>0$ predicted earlier,¹⁴ has been seen recently by Limelette *et al.*¹⁴ and by Kagawa *et al.*¹⁴ for the two-dimensional organic systems.

The Kondo insulator-NFL metal critical behavior is not hampered appreciably by the presence of magnetism in the latter phase, at least in the temperature range studied in this paper. Also, the insulating state is nonmagnetic. Therefore, the critical behavior at the KI-NFL boundary can be studied systematically as a function of x . Obviously, the situation drawn in the lower right-hand corner of Fig. 11 comprises the KI state as a *band* insulator for $x=0$ (with an even number of electrons), which appears naturally in the mean-field treatment of the Anderson lattice.^{8,9} The robust character of the KI state for nonstoichiometric samples ($0 < x < 0.12$) speaks in favor of incorporating the feature drawn in Fig. 5(b) i.e., in the favor of a true periodic Kondo-lattice singlet state for $0.13 > x > 0$. The KI-NFL transition will be characterized semiquantitatively next.

B. A simple theoretical model of KI metallization

As said above, a theoretical picture requires an incorporation of both the band-insulator features shown in Fig. 5(a) (even number—18 of valence electrons¹ including one $4f$ electron due to Ce, for CeRhSb), and the Kondo-lattice spin-singlet correlations^{8,9} shown in Fig. 5(b). Therefore, we take the view that $4f$ electrons due to Ce are even in the sample with $x \leq 0.12$ itinerant in the temperature regime $T_m \leq T \leq T_{max}$, but acquire also both the Kondo and the antiferromagnetic f - f correlations. Therefore, we start from the effective model represented by the following Hamiltonian:

$$H = - \sum_{\langle ij \rangle \sigma} t_{fj} f_{i\sigma}^\dagger f_{j\sigma} + \sum_i J_K (\mathbf{S}_{if} \cdot \mathbf{s}_{ic} - \frac{1}{4} n_{if} n_{ic}) + \sum_{ij} J_{ij} (\mathbf{S}_i \cdot \mathbf{S}_j - \frac{1}{4} n_{if} n_{jf}) + K \sum_i n_{if} n_{ic} + \epsilon_c. \quad (1)$$

The first term describes the hopping of f electrons between the nearest neighbors (NN) $\langle i, j \rangle$ with the hopping integral t_f , where $n_{f\sigma} = \langle f_{i\sigma}^\dagger f_{i\sigma} \rangle$ is the average number of f electrons per Ce atom and of spin σ , and the f -level occupancy is $n_f = n_{f\uparrow} + n_{f\downarrow} \leq 1$. The second term describes the local Kondo interaction between the f -electron spins $\{\mathbf{S}_{if}\}$ and the conduction electrons $\{\mathbf{s}_{ic}\}$ (the full exchange term involves also the part involving the number of f electrons $n_{if} = \sum_{\sigma} f_{i\sigma}^\dagger f_{i\sigma}$ and that of carriers n_{ic} , both for the site i). The third term describes the antiferromagnetic exchange interaction between f electrons. The fourth and the fifth terms describe, respectively, the direct interorbital Coulomb interaction and the conduction-band energy. The derivation of the model is outlined in Appendix A.

This model was obtained from the extended Anderson lattice model for $n_f \leq 1$ when the intraatomic f - f interaction with magnitude $U \sim 5 \div 6$ eV represents the largest energy scale in the system. In our system $J_{ex} z \lesssim J_K$, where z is the number of the NN, for which $J_{ij} \equiv J_{ex}$. Therefore, the three physical processes: band character of f electrons, as well as both the local Kondo (f - c), and (f - f) couplings are roughly of the same magnitude. This is because $T_{max} \sim 3 \div 4 T_m$. One should also mention that in the metallic phase Ruderman-Kittel-Kasuya-Yosida (RKKY)-type interaction appears in addition to the (short-range) antiferromagnetic kinetic-exchange interaction. From a theoretical point of view, such a situation presents itself as a highly nonperturbational problem. Therefore, to make simple estimates, we follow the spirit of the Gutzwiller variational approach,¹⁶ albeit simplified to a large extent by retaining only the principal qualitative features of the method.

We introduce the correlation functions $\langle \mathbf{S}_{if} \cdot \mathbf{s}_{ic} - \frac{1}{4} n_{if} n_{ic} \rangle$ and $\langle \mathbf{S}_{if} \cdot \mathbf{S}_{jf} - \frac{1}{4} n_{if} n_{jf} \rangle$ and regard them as the processes restricting the f -electron hopping, since the first prefers formation of a local singlet ($0 < \lambda \leq 1$), whereas the other—the appearance of the short-range antiferromagnetic correlations ($0 < m \leq 1$). In other words, in direct relation with the f - f hopping suppression by the Hubbard correlation ($q_\sigma < 1$), we introduce two additional band-narrowing factors due to these magnetic correlations. In effect, by taking into account the occupancies of the corresponding states, i.e., by assuming

In the undoped *Kondo insulating state* we must have $\lambda=1$ and $n=2$ (even number of valence electrons). In that state the intersite exchange interaction does not matter as we have Kondo singlets, so one can put $J_{ex}=0$. In that limit, we reach a very simple limiting value of (9), namely $n_f=1$. So, as conjectured on the basis of the experimental results, the f electrons in $\text{CeRh}_x\text{Sb}_{1-x}$ should be localized. In other words, the situation represented in Fig. 5(b) represents the limiting situation of that drawn in Fig. 5(a) when $n_f \rightarrow 1$.

The next question is what happens if we start doping the system? In that case the carrier concentration is diminished by replacing Sn for Sb. Then we can assume that $n=2-x$ (one conduction electron less per Sn atom) and keeping $\lambda=1$, and neglecting still the intersite exchange we have that

$$n_f \approx 1 - \frac{W/4 + (J_K - K)/2}{W/4 + J_K - K} x. \quad (10)$$

Thus, the valency of Ce is increased rapidly from the Ce^{3+} to $\text{Ce}^{(4-n_f)+}$ with the Sn doping. This tendency towards itinerancy of f electrons must be enhanced by the Kondo single disappearance, i.e., the condition $\lambda = \frac{1}{4}$. Then we have

$$n_f = \frac{1}{2} \frac{t_f z + (J_K/4 - K)(2-x) + (W/2)(1-x)}{t_f z + J_K/4 - K + 2J_{ex} z m + W/4}. \quad (11)$$

A simple numerical estimate for $m=1/4$ shows now that $1/2 < n_f < 1$, i.e., we have the mixed-valent situation at the Kondo-insulator instability threshold. Obviously, such a reasoning carried out for $T=0$ will not be able to provide a quantum-critical behavior, as it involves the generalization to $T>0$. Nonetheless, it supports clearly the qualitative picture drawn from the experimental results. Numerical details, involving analysis as a function of the five parameters (t_f , W , J_K , J_{ex} , and n), as well as their relation to the parameters of Anderson-lattice-Hamiltonian parameters (ϵ_f , U , V , cf. Appendix), should be provided separately.

One more important remark from the above analytical reasoning should be added. Namely, these considerations provide a supplement to the Doniach scenario, as they involve explicitly the itinerant nature of the heavy quasiparticles, caused by the f - c hybridization V and by the circumstance that $n_f < 1$.

VII. CONCLUDING REMARKS

In this paper we have provided a detailed discussion of the properties in the region of Kondo insulator—non-Fermi (non-Landau) liquid transition. The transition is discussed as a function of variable valence-electron number introduced by substitution of Sn for Sb. The results were compared with those for Mott-Hubbard localization-delocalization transition. It is important to note that we distinguish between the binding into the Kondo-lattice singlet of $4f$ electrons (as seen in the magnetic-susceptibility maximum position T_m) as distinct from the valence electrons [as characterized by the value of the gap $2\Delta(x)$].

The Kondo insulators $\text{CeRhSb}_{1-x}\text{Sn}_x$ (stable for $x \leq 0.12$) are here nondegenerate semiconductors with the almost constant activated carrier mobility. In this respect, they are

electrically similar to the Mott-Hubbard insulators $(\text{V}_{1-x}\text{Cr}_x)_2\text{O}_3$, even though the latter are antiferromagnetic semiconductors.^{16,17} We think that the temperature independence of the carrier mobility should be reflected upon further.

We have also proposed that the $4f$ electrons become localized in the KI phase as $T \rightarrow 0$. The critical behavior for $x > 0.12$ is highly nonstandard, since the equilibrium properties such as the magnetic susceptibility (both ac and dc) shows a divergent behavior in the whole range of concentrations ($x < 0.20$), in which the metallic samples can be synthesized. The extension of the experimental results to lower temperatures seems to be important and will be carried out in the near future. Also, the effect of the substitutional disorder, particularly for $x \geq 0.06$, should be studied carefully. Such a study should clarify the role of disorder (if any) in the Kondo-gap formation.

Finally, we have proposed an effective f -band model of correlated f electrons, which localize in the pure Kondo-insulating limit (the case of $\text{CeRh}_x\text{Sb}_{1-x}$). The model, in our view, catches salient features of the system evolution with varying carrier concentration and supplements the Doniach picture of the Kondo-lattice \rightarrow correlated (magnetic) metal transition.

ACKNOWLEDGMENTS

J.S. is grateful to the Ministry of Science and Information Technology for Grant No. 1 P03P 01 29. Two of the authors (A.Ś. and J.G.) acknowledge the support of the State Committee for Scientific Research (KBN), through Grant No. 1 P03B 052 28. J.S. acknowledges also the Polish Foundation for Science for funding during the years 2003–2006. The authors are also very grateful to Hilbert von Löhnyessen, Piers Coleman, and John Mydosh for critical remarks and comments. The technical help of Dr. Robert Podsiadły is appreciated. The work is partly carried out under the auspices of the COST P-16 European network entitled “Emergent Behaviour in Correlated Matter.”

APPENDIX: EFFECTIVE NARROW f -BAND MODEL OF CORRELATED AND HYBRIDIZED ELECTRONS

In this Appendix we outline the derivation of the effective narrow f -band model of correlated and almost localized electrons ($n_f \rightarrow 1$). For the sake of clarity, we neglect the orbital degeneracy of the $4f^1$ configuration of Ce and start with the extended Anderson lattice Hamiltonian with the intrasite hybridization only, which has the form

$$H = \sum_{\mathbf{k}\sigma} \epsilon_{\mathbf{k}} c_{\mathbf{k}\sigma}^\dagger c_{\mathbf{k}\sigma} + \sum_i \epsilon_f a_{i\sigma}^\dagger a_{i\sigma} + \frac{V}{\sqrt{N}} \sum_{i\mathbf{k}\sigma} (a_{i\sigma}^\dagger c_{\mathbf{k}\sigma} e^{i\mathbf{k}\cdot\mathbf{R}_i} + \text{H.c.}) + U \sum_i n_{if} n_{i\bar{f}} + \frac{U_{cf}}{N} \sum_{i\mathbf{k}\mathbf{k}'\sigma\sigma'} n_{if\sigma} c_{\mathbf{k}\sigma}^\dagger c_{\mathbf{k}'\sigma'} e^{i(\mathbf{k}'-\mathbf{k})\cdot\mathbf{R}_i}, \quad (\text{A1})$$

where $n_{if\sigma} = a_{i\sigma}^\dagger a_{i\sigma}$. The first term is the band energy of conduction (c) electrons. The second term is the atomic energy of f electrons (it is selected relative that for $5d-6s$ elec-

trons). The third term defines intra-atomic hybridization between the $5d-6s$ and $4f$ electrons, whereas the last two terms describe the intra-atomic Coulomb interactions, the $f-f$ and the $f-c$, respectively.

When speaking about the Kondo-lattice limit, we are thinking about the limit with appreciable Kondo coupling, but in general, with itinerant f electrons ($n_f < 1$). In this limit, we can transform out¹⁸ only the part of the hybridization term responsible for the formation of double f -level occupancies as they are realized only via virtual transitions, since $|V|/U \ll 1$. In effect, we obtain the following effective Hamiltonian in the second order in V in the real-space representation:

$$\begin{aligned} \tilde{H} = & \sum_{mn\sigma} t_{mn} c_{m\sigma}^\dagger c_{n\sigma} + \epsilon_f \sum_{i\sigma} n_{if\sigma} + U \sum_i n_{if\uparrow} n_{if\downarrow} + U_{cf} \sum_i n_{if} n_{ic} \\ & + V \sum_{i\sigma} [f_{i\sigma}^\dagger (1 - n_{if\bar{\sigma}}) c_{i\sigma}^\dagger + \text{H.c.}] \\ & + \sum_i \frac{2V^2}{U - U_C + \epsilon_f} (\mathbf{S}_{if} \cdot \mathbf{s}_{ic} - \frac{1}{4} n_{if} n_{ic}) + \dots, \end{aligned} \quad (\text{A2})$$

where $n_{if} = \sum_{\sigma} n_{if\sigma}$, $n_{ic} = \sum_{\sigma} c_{i\sigma}^\dagger c_{i\sigma}$, and \mathbf{S}_{if} and \mathbf{s}_{ic} are, respectively, the spin operators for f and c electrons in the fermion representation. Note that due to the itineracy of f electrons, we cannot transform out the whole hybridization term, as in such a situation the number of f and c electrons would be conserved separately¹⁹ and the hybridized $f-c$ states would not be formed. In other words, the full Schrieffer-Wolff transformation¹⁹ viewed as a two-step procedure cannot be carried out if we would like to discuss a heavy-fermion or mixed-valent states, both of which require noninteger f -atom valency ($n_f < 1$).

In order to solve the Hamiltonian (A2), one can use the slave-boson approximation,^{4,8,9} which leads to the renormalized quasiparticle states represented in the simplest case by the Hamiltonian

$$\begin{aligned} \tilde{H} = & \sum_{mn\sigma} t_{mn} c_{m\sigma}^\dagger c_{n\sigma} + \tilde{\epsilon}_f \sum_{i\sigma} n_{if\sigma} + V \sum_{i\sigma} q^{1/2} (f_{i\sigma}^\dagger c_{i\sigma} + c_{i\sigma}^\dagger f_{i\sigma}) \\ & + J_K n_f n_c \sum_i (\tilde{\mathbf{S}}_i \cdot \tilde{\mathbf{s}}_i - \frac{1}{4}) + U_C \sum_i n_{if} n_{ic} + \dots, \end{aligned} \quad (\text{A3})$$

where $J_K = V/(U - U_C + \epsilon_f)$, q_σ is the renormalization factor, which can also be obtained in the Gutzwiller approximation and in $U \rightarrow \infty$ limit reads $q_\sigma = (1 - n_f)/(1 - n_{f\sigma})$. Also the effective fermionic operators for the f states are $f_{i\sigma}^\dagger$ and $f_{i\sigma}$

(also, now $n_{if\sigma} \equiv f_{i\sigma}^\dagger f_{i\sigma}$). $\tilde{\epsilon}_f$ is the renormalized f -level position.

In the $U \rightarrow \infty$ limit $J_K \rightarrow 0$ and Hamiltonian (A3) can be easily diagonalized leading the renormalized quasiparticle energies $E_{\mathbf{k}\alpha}$ of the form

$$E_{\mathbf{k}\alpha} = \frac{\epsilon_{\mathbf{k}} - \tilde{\epsilon}_f}{2} + \alpha \left[\left(\frac{\epsilon_{\mathbf{k}} - \tilde{\epsilon}_f}{2} \right)^2 + \tilde{V}_\sigma^2 \right]^{1/2}, \quad (\text{A4})$$

where $\alpha = \mp 1$ for bonding and antibonding hybridized bands, respectively, and $\tilde{V}_\sigma = q_\sigma V$.

The Kondo-lattice state is understood in this language as the limit for which for the filled states $|\tilde{V}_\sigma/(\epsilon_f - \mu)| \ll 1$. In that limit, the effective narrow-band part ($\alpha = -1$) reduces to

$$E_{\mathbf{k}\sigma} \simeq \Theta^2 \epsilon_{\mathbf{k}} + \text{const}, \quad (\text{A5})$$

with $\Theta = -V^2/|\epsilon_f|q$. In effect, the f electrons acquire a non-zero bandwidth $\sim V^2 q$; and their propagation between the neighboring pair of sites $\langle i, j \rangle$ is composed of three steps $f \rightarrow c$ transition at site i , propagation from the site i to j as a conduction electron followed by $c \rightarrow f$ transition at site j . Such a propagation is possible only if $n_f < 1$, i.e., when the valency is noninteger. As shown in Sec. VI, the system is not in a pure Kondo insulating state.

Summing up the whole argument, allowing for $U < \infty$, including the Kondo-like term ($J_K > 0$ now), as well as adding the $f-f$ exchange interaction term which appears in the fourth order, we arrive at the effective narrow f band of correlated electrons in the form

$$\begin{aligned} \tilde{H} = & \sum_{ij\sigma} q_\sigma t_{ij} f_{i\sigma}^\dagger f_{j\sigma} + \tilde{\epsilon}_f \sum_{i\sigma} f_{i\sigma}^\dagger f_{i\sigma} + U_C \sum_i n_{if} n_{ic} \\ & + J_K n_f n_c \sum_i (\tilde{\mathbf{S}}_i \cdot \tilde{\mathbf{s}}_i - \frac{1}{4}) + \sum_{i \neq j} J_{ij} n_f^2 (\tilde{\mathbf{S}}_i \cdot \tilde{\mathbf{S}}_j - \frac{1}{4}) + \epsilon_c, \end{aligned} \quad (\text{A6})$$

where now $t_{ij} = t_{mn} V^2 |\epsilon_f|$ with $(m, n) = \langle i, j \rangle$, $J_K = V^2/|\epsilon_f|(\epsilon_f + U - U_C)$, J_{ij} being the $f-f$ interaction magnitude and $\tilde{\epsilon}_f \equiv k_B T_K$ —the effective f -level position. This is the starting Hamiltonian for a further analysis. It is analyzed further in Sec. VI. Let us only note that the operators $\tilde{\mathbf{S}}_i$ and $\tilde{\mathbf{s}}_i$ are the atomic (Pauli) representation of the corresponding spins, since n_f and n_c represent the occupancies of the f and c states at given sites. Also, the conservation of the electron number is enforced through the condition $n_f + n_c = n$, where n is the average number of electrons per pair of $f-c$ states (per formula unit in the simplest case).

¹A. Ślebarski and J. Spałek, Phys. Rev. Lett. **95**, 046402 (2005).

²G. R. Stewart, Rev. Mod. Phys. **73**, 797 (2001); see also articles in J. Phys.: Condens. Matter **8**, No. 48 (1996); D. M. Newns and N. Read, Adv. Phys. **36**, 799 (1987).

³Z. Fisk, D. W. Hess, C. J. Pethick, D. Pines, J. L. Smith, J. D. Thompson, and J. O. Willis, Science **239**, 33 (1988); for a recent overview see P. Coleman and A. J. Schofield, Nature

(London) **433**, 226 (2005), and references therein; Q. Si, S. Rabello, K. Ingersent, and J. L. Smith, *ibid.* **413**, 804 (2001).

⁴P. A. Lee, T. M. Rice, J. W. Serene, L. J. Sham, and J. W. Wilkins, Comments Condens. Matter Phys. **12**, 99 (1986).

⁵For a general review see: F. Gebhard, *The Mott Metal-Insulator Transition*, 2nd ed. (Springer-Verlag, Berlin, 1997). The quantum criticality in the context of narrow-band physics is studied

- mainly at the magnetic-paramagnetic phase transition at $T=0$; see: J. Hertz, Phys. Rev. B **14**, 1165 (1976); A. J. Millis, *ibid.* **48**, 7183 (1993); T. Moriya, *Spin Fluctuations in Itinerant Electron Magnetism* (Springer-Verlag, Berlin, 1985).
- ⁶P. Fulde, J. Keller, and G. Zwicknagl, *Theory of Heavy Fermion Systems*, Solid State Physics Vol. 41 (Academic Press, New York, 1988), p. 1; J. Spałek, *Fermi Liquids and Their Localization*, edited by F. Bassani *et al.* (Elsevier, Amsterdam, 2005), Vol. 3, pp. 126–36; P. Coleman, C. Pépin, Qimio Si, and R. Ramazashili, J. Phys.: Condens. Matter **13**, R723 (2001).
- ⁷P. Nozieres, Ann. Phys. (Paris) **10**, 19 (1985); Eur. Phys. J. B **6**, 447 (1998).
- ⁸R. Doradziński and J. Spałek, Phys. Rev. B **56**, R14239 (1997); **58**, 3293 (1998).
- ⁹For review see: J. Spałek, and R. Doradziński, in *Magnetism and Electronic Correlations in Local-moment Systems: Rare Earth Elements and Compounds*, edited by M. Donath, P. A. Dowben and W. Nolting (World Scientific, Singapore, 1998), p. 387; Acta Phys. Pol. A **96**, 677 (1999).
- ¹⁰A. Ślebarski, T. Zawada, J. Spałek, and A. Jezierski, Phys. Rev. B **70**, 235112 (2004), and references therein.
- ¹¹B. C. Sales and D. Wohlleben, Phys. Rev. Lett. **35**, 1240 (1975).
- ¹²S. Doniach, Physica B & C **91**, 231 (1977); B. H. Bernhard, C. Lacroix, J. R. Iglesias, and B. Coqblin, Phys. Rev. B **61**, 441 (2000).
- ¹³S. Gabàni, E. Bauer, S. Berger, K. Flabchart, Y. Paderno, C. Paul, V. Pavlik, and N. Shitsevalova, Phys. Rev. B **67**, 172406 (2003).
- ¹⁴J. Spałek, A. Datta, and J. M. Honig, Phys. Rev. Lett. **59**, 728 (1987); P. Limelette, A. Georges, D. Jérôme, P. Wzietek, P. Mecalif, and J. M. Honig, Science **302**, 89 (2003); F. Kagawa, K. Miyagawa, and K. Kanoda, Nature (London) **436**, 534 (2005).
- ¹⁵J. M. Honig and J. Spałek, Chem. Mater. **10**, 2910 (1999); X. Yao, J. M. Honig, T. Hogan, C. Kannewurf and J. Spałek, Phys. Rev. B **54**, 17469 (1996).
- ¹⁶J. Spałek (unpublished).
- ¹⁷H. Kuwamoto, J. M. Honig, and J. Appel, Phys. Rev. B **22**, 2626 (1980).
- ¹⁸J. Spałek and P. Gopalan, J. Phys. (France) **50**, 2869 (1989).
- ¹⁹J. R. Schrieffer and P. A. Wolff, Phys. Rev. **149**, 491 (1966); for a review of two-step procedure see: J. Spałek and J. M. Honig, in *Studies of High Temperature Superconductors*, edited by A. Narlikar (Nova Science, New York, 1991), pp. 1–64.